nature photonics

LETTERS

PUBLISHED ONLINE: 23 JUNE 2013 | DOI: 10.1038/NPHOTON.2013.150

Quantum-dense metrology

Sebastian Steinlechner, Jöran Bauchrowitz, Melanie Meinders, Helge Müller-Ebhardt, Karsten Danzmann and Roman Schnabel*

Quantum metrology utilizes entanglement to improve the sensitivity of measurements[1–3]. To date, the focus has been on the measurement of a single observable. Its orthogonal observable, however, may contain additional information, the knowledge of which can be used to further improve the measurement result beyond what is possible with state-of-the-art quantum metrology. Here we demonstrate a laser interferometer that provides information about two non-commuting observables, with uncertainties below the meter's quantum ground state. Our experiment is a proof of principle of what we call 'quantum-dense metrology', referring to its increased measurement information and its analogy to quantum-dense coding in quantum information science. We propose to use the additional information to discriminate between the actual science signal and parasitic signals originating from scattered photons. Our approach can be readily applied to improve squeezed-light enhanced gravitational-wave detectors at non-quantum noise-limited detection frequencies by providing a sub-shot-noise veto trigger against stray-light-induced signals.

The Heisenberg uncertainty principle (HUP) limits the amount of information that can be obtained about non-commuting observables of a physical system. Prominent examples are the position and momentum of a particle or the amplitude and phase quadratures of an electromagnetic wave. To optimize the sensitivity of a measurement device under given constraints, such as limited energy, this limit demands a sophisticated design of the 'meter' (or 'probe') system (which couples to the targeted measurement quantity) as well as a sophisticated design of the detector that reads out the meter observable, which is an (optimal) estimator of the measurement quantity[1,4]. Non-classical meter states have been used to 'squeeze' the imprecision in one meter observable to below its zero-point fluctuation, entering the regime of quantum metrology. The first such experiments were applied to squeezed-light enhanced laser-interferometric phase measurements[3]. Further examples include phase measurements with entangled photons[5–7], entangled ions[8] and non-classical states of neutral atoms[9,10], entanglement-assisted nuclear magnetic resonance[11] and magnetometry with entangled magnetic moments of atomic ensembles[12]. Recently, quantum metrology has been applied to improve an operating gravitational wave detector (GWD)[13].

All previous experiments in quantum metrology aimed to improve the signal-to-noise ratio of a single meter observable. However, the meter's orthogonal observable may contain additional information with a different physical origin. To date, a simultaneous quantum measurement of additional, independent (incoherent) information encoded in the meter's orthogonal observable has not been considered. In general, when using a single, separable and squeezed meter mode, the HUP demands increased ('anti-squeezed') quantum noise in the orthogonal observable, which prohibits a simultaneous non-classically improved readout of both observables.

Here we propose and implement the concept of quantum-dense metrology (QDM), which qualitatively increases the measurement information compared to conventional quantum metrology by simultaneously reading out two conjugate observables. Both observables show squeezed quantum noise and act as estimators of independent physical quantities.

QDM is based on an Einstein–Podolsky–Rosen (EPR) entangled[14] two-mode system, first proposed for metrology by D'Ariano and colleagues[15]. One mode of the entangled system, described by the bosonic annihilation operator $\hat{a}_\mathrm{m}$, serves as the new meter state, whereas the other mode $\hat{a}_\mathrm{r}$ is kept as an external reference for the measurement device (Fig. 1). In principle, it is possible to measure exactly the distance in phase space between the two modes, because the difference in their canonical positions $\hat{x}_\mathrm{m} - \hat{x}_\mathrm{r}$ and the sum of their canonical momenta $\hat{p}_\mathrm{m} + \hat{p}_\mathrm{r}$ commute, $[\hat{x}_\mathrm{m} - \hat{x}_\mathrm{r}, \hat{p}_\mathrm{m} + \hat{p}_\mathrm{r}] = 0$, where $\hat{x}_\mathrm{m,r} = (\hat{a}_\mathrm{m,r} + \hat{a}^\dagger_\mathrm{m,r})/\sqrt{2}$ and $\hat{p}_\mathrm{m,r} = -i(\hat{a}_\mathrm{m,r} - \hat{a}^\dagger_\mathrm{m,r})/\sqrt{2}$. We overcome the limitation set by the Heisenberg uncertainty relation (HUR) for reading out two orthogonal quadratures of a system by performing all measurements in relation to the reference beam. This situation was recently described as 'quantum-mechanics free'[16]. The required (continuous-variable) entangled states were first demonstrated by Ou *et al.*[17] and subsequently by many other groups[18–20]. They were previously considered for the quantum-informational task of dense coding, which doubles the capacity of quantum communication channels[21,22]. In contrast to all previously discussed applications of EPR entanglement, QDM benefits from two-mode squeezing of non-orthogonal quadratures. Our discussion shows that this opens a way to optimize the science-signal-to-noise ratio within QDM.

The measurement problem of reading out two orthogonal quadratures was first discussed by Arthurs and Kelly[23]. Consider an optical field described by the position and momentum-like quadrature amplitudes $\hat{x}$ and $\hat{p}$. Two physical interactions $U(t)$ and $U'(t)$ modulate the field, resulting in incoherent, classical amplitude and phase signals $X = \langle\hat{x}\rangle$ and $P = \langle\hat{p}\rangle$. From the commutation relation $[\hat{x}, \hat{p}] = i$, one obtains the signal-normalized HUR

$$\frac{\Delta^2\hat{x}}{|X|^2}\frac{\Delta^2\hat{p}}{|P|^2} \geq \frac{1}{4|X|^2|P|^2} \tag{1}$$

where the quadrature variances for the ground state are normalized to $\Delta^2\hat{x} = \Delta^2\hat{p} = 1/2$. However, actually measuring both quadratures of a separable mode simultaneously (subscript 'sim') with, for example, an eight-port homodyne detector[24] leads to an uncertainty product that is four times as large[23]:

$$\frac{\Delta^2\hat{x}_\mathrm{sim}}{|X_\mathrm{sim}|^2}\frac{\Delta^2\hat{p}_\mathrm{sim}}{|P_\mathrm{sim}|^2} \geq \frac{1}{|X|^2|P|^2} \tag{2}$$

Institut für Gravitationsphysik, Leibniz Universität Hannover and Max-Planck-Institut für Gravitationsphysik (Albert-Einstein-Institut), Callinstrasse 38, 30167 Hannover, Germany. *e-mail: roman.schnabel@aei.mpg.de

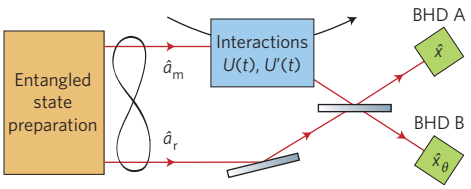

Figure 1 | Schematic showing the underlying principle of QDM. The measurement uses a bipartite (continuous-variable) entangled state; one part (the 'meter') probes two different interactions $U(t)$ and $U'(t)$ and the other part is kept as an external reference. When leaving the interaction zone the meter mode, which is described here by the annihilation operator $\hat{a}_m$, carries two pieces of information encoded in two non-commuting observables. Both pieces of information are extracted with squeezed quantum noise by recombining the entangled modes on a beamsplitter and by detecting different observables (using two balanced homodyne detectors).

With QDM, the simultaneous readout is no longer limited by such an uncertainty relation. Instead, the achievable sensitivity is directly connected to the squeezing parameters r_a, r_b of the initial squeezed beams. Overlapping them with a relative angle θ on a beamsplitter produces entanglement and allows for a simultaneous detection of the quadrature $\hat{x}$ and the rotated quadrature $\hat{x}_\theta = \hat{x}\cos\theta + \hat{p}\sin\theta$ with

$$\frac{\Delta^2\hat{x}^{\mathrm{ent}}_{\mathrm{sim}}}{|X_{\mathrm{sim}}|^2}\frac{\Delta^2\hat{x}^{\mathrm{ent}}_{\theta,\mathrm{sim}}}{|X_{\theta,\mathrm{sim}}|^2} \geq \frac{e^{-2r_a}e^{-2r_b}}{|X|^2|X_\theta|^2} \qquad (3)$$

Setting $\theta = \pi/2$, the fundamental improvement compared to the lower bound in inequality (2) becomes obvious. The HUR (equation (1)) for a conventional readout based on a single separable mode is surpassed for two-mode squeezing if $r_{a,b} > 0.347$. A detailed derivation of the above results can be found in the Supplementary Information.

In this work we experimentally proved the principle of QDM and its high potential for improving state-of-the-art laser interferometers. Our set-up (Fig. 2) is in direct analogy to Fig. 1. We first generated entangled light from two squeezed modes, following earlier work[18]. One mode of the entangled state was mode-matched into the output port of a Michelson-type laser interferometer operating at its dark fringe (Fig. 2). The actual interferometer phase signal was produced by modulating the piezoelectric transducer (PZT)-mounted north-arm mirror at 5.55 MHz. We intentionally introduced a parasitic signal at 5.17 MHz by PZT-modulating a small amount of light that leaked through the east-arm mirror. By adjusting the phase of the light that is back-reflected into the interferometer, we were able to simulate a parasitic interference in any quadrature. Such a disturbance occurs naturally in any measurement device due to rescattering of meter state quanta from moving surfaces[25]. A more detailed explanation of the experimental set-up is given in the Methods.

The results of our experiment are presented in Fig. 3. Each point in the spectra corresponds to the noise power of an operator, $\hat{x} = \hat{x}(\Omega, \Delta\Omega)$, where $\Delta\Omega$ is the spectral width defined by the resolution bandwidth set at the spectral analyser (10 kHz in our case). The non-classical sensitivity improvement in Fig. 3a is ~6 dB ($r_a \approx 0.69$). At the same time, the interferometer's sensitivity in the orthogonal quadrature $\hat{p}$ (Fig. 3b) is also ~6 dB better than in the classical case ($r_b \approx 0.69$). Figure 3a,b clearly surpasses the limit set by inequality (2), and even outperforms inequality (1).

QDM uses the simultaneous squeezing in two orthogonal quadratures to improve the overall measurement, here by identifying a parasitic (disturbance) signal, as described in the following. Balanced homodyne detector (BHD) A measures the amplitude quadrature (Fig. 3a, orange trace), which generally provides the highest signal-to-noise ratio for the interferometric science signal (here at 5.55 MHz). BHD A also clearly detects a second (parasitic) signal at 5.17 MHz. Looking at $\hat{p}$ with BHD B (Fig. 3b), the phase signal at 5.55 MHz vanishes as expected, while the signal at 5.17 MHz does not vanish but actually increases in size. This information is sufficient to reveal the parasitic nature of the lower frequency signal, which can thus be excluded ('vetoed') from further data analysis.

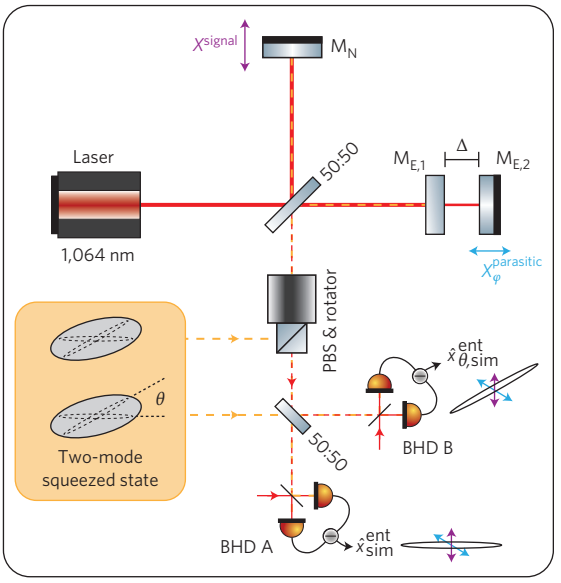

Figure 2 | Schematic set-up for the experimental demonstration of QDM. Inside a Michelson interferometer, two independent interactions $U^{\mathrm{signal}}(t)$ and $U^{\mathrm{parasitic}}(t)$ are generated by the PZT-driven mirrors M_N and $M_{E,2}$. They result in a 'scientific' signal X^{signal} and a disturbance signal $X^{\mathrm{parasitic}}_{\varphi}$. X^{signal} corresponds to a pure amplitude modulation of the interferometer output beam, while $X^{\mathrm{parasitic}}_{\varphi}$ describes a modulation that is rotated into quadrature angle φ by adjusting Δ, which is the microscopic spacing between the east mirrors. A Faraday rotator in combination with a polarizing beamsplitter (PBS) couples one part of the entangled state into the interferometer. The other part is overlapped with the light beam leaving the interferometer. The two resulting beams are simultaneously detected with balanced homodyne detectors BHD A and B, which measure quadratures $\hat{x}$ and $\hat{x}_{\theta\neq 0}$, respectively $\hat{p} \equiv \hat{x}_{\theta=\pi/2}$. The total projected signal at BHD A reads $X_{\mathrm{sim}} = (1/\sqrt{2})(X^{\mathrm{signal}} + X^{\mathrm{parasitic}}_{\varphi}\cos\varphi)$.

In Fig. 3c, we used an improved strategy to reveal the parasitic signal. We detuned the angle θ between the original squeezing ellipses away from 90°. In this way it is possible to retain at least part of the science signal in BHD B, while still having insight into the orthogonal quadrature. As the projection of a phase signal measured at BHD A into the $\hat{x}_\theta$ quadrature can be calculated exactly, any discrepancy reveals a parasitic signal. The dashed black lines in Fig. 3b,c show the projected noise power, assuming that Fig. 3a contains only phase signals. Although the signal at 5.55 MHz perfectly matches the expectation, the disturbance at 5.17 MHz clearly does not. The advantage of the measurement in Fig. 3c is that, together with Fig. 3a, the overall signal-to-noise ratio of the science signal is improved.

In the following we discuss the application of QDM in state-of-the-art measurement devices. Generally, to achieve high quantum-noise-limited sensitivities, very bright states have to be used. Current laser-interferometric GWDs use light fluxes of $\sim 1 \times 10^{20}$ photons per second[26]. Just a single photon per second and hertz, which is backscattered from a vibrating surface and in this way frequency-shifted into the detection band, produces a significant parasitic interference signal. Such disturbances are a well-known

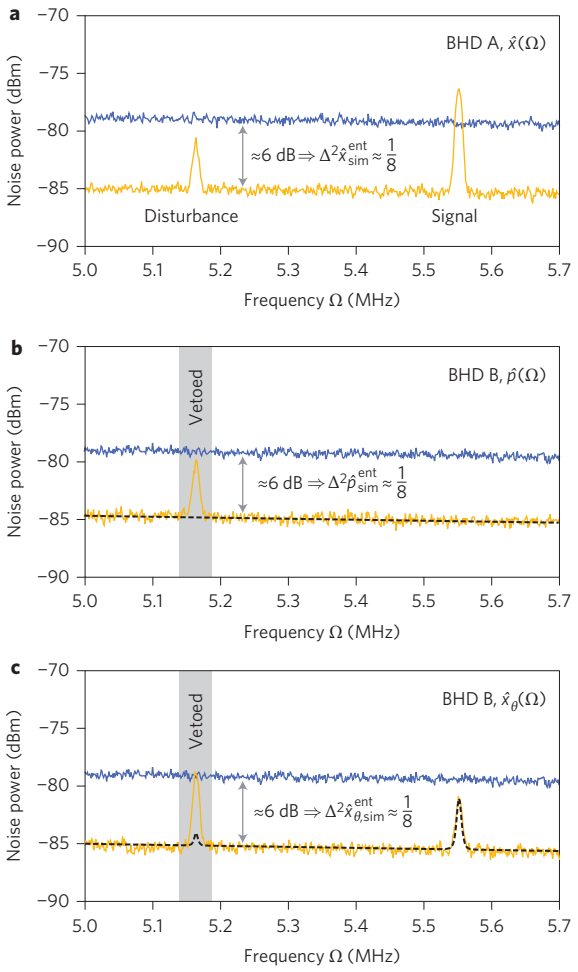

Figure 3 | Experimental demonstration of QDM. a–c, Orange traces show the (unnormalized) simultaneously squeezed quadrature noise-power spectra $\Delta^2\hat{x}(\Omega)$ (BHD A, **a**) and $\Delta^2\hat{p}(\Omega)$ or $\Delta^2\hat{x}_\theta(\Omega)$ (BHD B, **b** and **c**, respectively) in comparison with the respective spectra of the meter's zero-point fluctuations (blue). In **b** and **c**, parasitic signals due to their unexpected scaling can be observed. The calculated scalings of science signals are shown as the dashed black curves. In **c**, angle θ was tuned so that part of the true science signal was recovered. All traces are slightly sloped due to the decreasing transfer function of the homodyne detectors. They were recorded with a resolution bandwidth of $\Delta\Omega = 10$ kHz, a video bandwidth of 100 Hz, and were averaged three times.

problem in high-precision laser interferometry[25,27,28] and are ultimately a fundamental problem in any measuring device aiming for high quantum-noise-limited sensitivities. We presume that the sensitivity limitation at lower detection frequencies in the squeezed-light enhanced GWD GEO 600 (ref. 13) at least partially originates from parasitic interferences. Using QDM in GEO 600, in direct analogy to Fig. 2, would allow us to clarify which of the (low-frequency) signals are parasitic and which occur in the quadrature where gravitational waves are expected.

In conclusion, we have introduced and experimentally demonstrated the concept of quantum-dense metrology. QDM makes use of entanglement to achieve a simultaneous non-classical readout of two conjugate observables, which are estimators for quantities originating from independent physical processes. Our approach uses steady-state entanglement and therefore does not rely on any kind of conditioning or post-selection, which would result in a loss of measurement time. For the first time we propose two-mode squeezing for metrology, generated with a non-orthogonal relative squeezing angle. Such entangled states allow optimization of the signal-to-noise ratio when QDM is applied.

We have shown experimentally that QDM is superior to conventional quantum metrology and can be used to distinguish between scientific and parasitic signals with a precision beyond the ground-state uncertainty. Although our application of QDM does not help in the case of parasitic signals that occur solely in the phase quadrature, for example caused by thermally excited fluctuations of mirror surfaces and radiation pressure forces, it is a valuable tool against all types of parasitic signals that have a phase space orientation different from the phase quadrature. It should even be possible to subtract parasitic signals from the measurement data without subtracting science signals. For this, the assumption has to be made that the temporal or spectral shapes of the science and parasitic signals are different. Then, fitting parameters could be introduced that describe with which magnitudes the parasitic signals are projected onto the conventional readout quadrature of the interferometer. Fitting parameters are already used in data analysis based on matched filtering and signal templates[29]. Beyond the identification of parasitic signals, QDM might find application in all measurement interactions where different physical processes interact independently with non-commuting observables of the meter system. We envision that QDM will widen the application of quantum metrology in ongoing and future high-precision measurements.

Methods

Entangled-light generation. Our continuous-variable entangled light was generated by a source as described in a previous publication[30]. Two squeezed vacuum fields generated by degenerate type I parametric downconversion in periodically-poled potassium titanyl phosphate (PPKTP) were overlapped at a 50:50 beamsplitter, thereby creating two-mode squeezed light. Both input fields carried a residual phase modulation from locking the optical parametric amplifiers. At the detection stage, this modulation was reused to align the homodyne detectors to the squeezed quadratures. A single sideband modulation was imprinted on one of the squeezed fields by overlapping it with 80 MHz frequency-shifted light from an acousto-optical modulator. This sideband was used to lock the quadrature angle between the input squeezed states. It was also used to stabilize one mode of the entangled field to the Michelson interferometer by detecting the beat signal between the sideband and the interferometer input field behind one end-mirror.

Interferometer set-up and control. The Michelson interferometer had an arm length of ~7.5 cm for the north arm. The east arm was ~1.5 cm shorter, which allowed us to use the so-called Schnupp modulation technique for locking the interferometer to its dark fringe. Both end-mirrors were flat and had power reflectivities of 99.98% (M_N) and 98% (M_{E1}). The north mirror was PZT-mounted to create a phase modulation inside the interferometer. A second PZT-mounted flat mirror M_{E2} with a reflectivity of ~20% was placed a few millimetres behind M_{E1}, creating a (weakly coupled) Fabry–Pérot cavity. By tuning this cavity, the phase signal created by M_{E2} could be rotated into an arbitrary quadrature. A d.c. locking scheme detected the transmitted light and held the cavity at its operating point. Both PZTs were driven on a mechanical resonance to create signals in the few-megahertz regime where the detected squeezing was strongest.

Received 15 November 2012; accepted 10 May 2013; published online 23 June 2013

References

1. Giovannetti, V., Lloyd, S. & Maccone, L. Quantum-enhanced measurements: beating the standard quantum limit. *Science* **306,** 1330–1336 (2004).
2. Giovannetti, V., Lloyd, S. & Maccone, L. Quantum metrology. *Phys. Rev. Lett.* **96,** 010401 (2006).
3. Schnabel, R., Mavalvala, N., McClelland, D. E. & Lam, P. K. Quantum metrology for gravitational wave astronomy. *Nat. Commun.* **1,** 121 (2010).
4. Kimble, H. J., Levin, Y., Matsko, A. B., Thorne, K. S. & Vyatchanin, S. P. Conversion of conventional gravitational-wave interferometers into quantum nondemolition interferometers by modifying their input and/or output optics. *Phys. Rev. D* **65,** 22002 (2001).
5. Rarity, J. *et al.* Two-photon interference in a Mach–Zehnder interferometer. *Phys. Rev. Lett.* **65,** 1348–1351 (1990).
6. Mitchell, M., Lundeen, J. & Steinberg, A. Super-resolving phase measurements with a multiphoton entangled state. *Nature* **429,** 161–164 (2004).
7. Afek, I., Ambar, O. & Silberberg, Y. High-NOON states by mixing quantum and classical light. *Science* **328,** 879–881 (2010).

8. Leibfried, D. *et al.* Toward Heisenberg-limited spectroscopy with multiparticle entangled states. *Science* **304,** 1476–1478 (2004).
9. Gross, C., Zibold, T., Nicklas, E., Estève, J. & Oberthaler, M. K. Nonlinear atom interferometer surpasses classical precision limit. *Nature* **464,** 1165–1169 (2010).
10. Lücke, B. *et al.* Twin matter waves for interferometry beyond the classical limit. *Science* **334,** 773–776 (2011).
11. Cappellaro, P. *et al.* Entanglement assisted metrology. *Phys. Rev. Lett.* **94,** 020502 (2005).
12. Wasilewski, W. *et al.* Quantum noise limited and entanglement-assisted magnetometry. *Phys. Rev. Lett.* **104,** 133601 (2010).
13. Abadie, J. *et al.* A gravitational wave observatory operating beyond the quantum shot-noise limit. *Nature Phys.* **7,** 962–965 (2011).
14. Einstein, A., Podolsky, B. & Rosen, N. Can quantum-mechanical description of physical reality be considered complete? *Phys. Rev.* **47,** 777–780 (1935).
15. D'Ariano, G. M., Lo Presti, P. & Paris, M. G. A. Using entanglement improves the precision of quantum measurements. *Phys. Rev. Lett.* **87,** 270404 (2001).
16. Tsang, M. & Caves, C. Evading quantum mechanics: engineering a classical subsystem within a quantum environment. *Phys. Rev. X* **2,** 031016 (2012).
17. Ou, Z. Y., Pereira, S. F., Kimble, H. J. & Peng, K. C. Realization of the Einstein–Podolsky–Rosen paradox for continuous variables. *Phys. Rev. Lett.* **68,** 3663–3666 (1992).
18. Furusawa, A. *et al.* Unconditional quantum teleportation. *Science* **282,** 706–709 (1998).
19. Silberhorn, C. *et al.* Generation of continuous variable Einstein–Podolsky–Rosen entanglement via the Kerr nonlinearity in an optical fiber. *Phys. Rev. Lett.* **86,** 4267–4270 (2001).
20. Bowen, W. P., Schnabel, R. & Lam, P. K. Experimental investigation of criteria for continuous variable entanglement. *Phys. Rev. Lett.* **90,** 043601 (2003).
21. Bennett, C. H. & Wiesner, S. J. Communication via one-and two-particle operators on Einstein–Podolsky–Rosen states. *Phys. Rev. Lett.* **69,** 2881–2884 (1992).
22. Braunstein, S. L. & Kimble, H. J. Dense coding for continuous variables. *Phys. Rev. A* **61,** 042302 (2000).
23. Arthurs, E. & Kelly, J. L. B.S.T.J. Briefs: On the simultaneous measurement of a pair of conjugate observables. *Bell Syst. Tech. J.* **44,** 725–729 (1965).
24. Leonhardt, U. *Measuring the Quantum State of Light* Ch. 6 (Cambridge Univ. Press, 1997).
25. Vahlbruch, H., Chelkowski, S., Danzmann, K. & Schnabel, R. Quantum engineering of squeezed states for quantum communication and metrology. *New J. Phys.* **9,** 371 (2007).
26. Abramovici, A. *et al.* LIGO: the laser interferometer gravitational-wave observatory. *Science* **256,** 325–333 (1992).
27. Vinet, J-Y., Brisson, V. & Braccini, S. Scattered light noise in gravitational wave interferometric detectors: coherent effects. *Phys. Rev. D* **54,** 1276–1286 (1996).
28. Ottaway, D. J., Fritschel, P. & Waldman, S. J. Impact of upconverted scattered light on advanced interferometric gravitational wave detectors. *Opt. Express* **20,** 8329–8336 (2012).
29. Sathyaprakash, B. & Schutz, B. Physics, astrophysics and cosmology with gravitational waves. *Living Rev. Relativity* **12,** 2 (2009).
30. Steinlechner, S., Bauchrowitz, J., Eberle, T. & Schnabel, R. Strong Einstein–Podolsky–Rosen steering with unconditional entangled states. *Phys. Rev. A* **87,** 022104 (2013).

Acknowledgements

The authors acknowledge discussions with T. Eberle, V. Händchen and H. Lück. This research was financed by the Deutsche Forschungsgemeinschaft (Sonderforschungsbereich Transregio 7, project C8), the European Union Seventh Framework Programme for Research (FP7), project 'Quantum Interfaces, Sensors and Communication based on Entanglement' (Q-ESSENCE), and supported by the Centre for Quantum Engineering and Space–Time Research (QUEST) and the International Max Planck Research School (IMPRS) on Gravitational Wave Astronomy.

Author contributions

R.S. developed the initial idea for this work. H.M-E. and S.S. contributed to the theoretical background. S.S., J.B. and R.S. conceived the experiment. S.S., J.B. and M.M. conducted the experiment under supervision from K.D. and R.S.

Additional information

Supplementary information is available in the online version of the paper. Reprints and permissions information is available online at www.nature.com/reprints. Correspondence and requests for materials should be addressed to R.S.

Competing financial interests

The authors declare no competing financial interests.